Journal of Computational and Applied Mathematics 234 (2010) 1258–1266

Contents lists available at ScienceDirect

Journal of Computational and Applied Mathematics

journal homepage: www.elsevier.com/locate/cam

A Hamiltonian-conserving Galerkin scheme for the Camassa–Holm equation☆

Takayasu Matsuo

Graduate School of Information Science and Technology, The University of Tokyo, Hongo 7-3-1, Bunkyo-ku, Tokyo, 113-0033, Japan

ARTICLE INFO

Article history:
Received 30 September 2008
Received in revised form 12 August 2009

MSC:
65M06

Keywords:
Galerkin method
Finite-element method
Conservation
Camassa–Holm equation

ABSTRACT

A new Hamiltonian-conserving Galerkin scheme for the Camassa–Holm equation is presented. The scheme has an additional welcome feature that in exact arithmetic it is unconditionally stable in the sense that the solution is always bounded. Numerical examples that confirm the theory and the effectiveness of the scheme are also given.

1. Introduction

In this paper we are concerned with the numerical computation of the so-called Camassa–Holm (CH) equation on a circle:

$$u_t - u_{xxt} + 3uu_x = 2u_xu_{xx} + uu_{xxx}, \quad x \in \mathbb{S},\ t > 0, \tag{1}$$

where $u(x, t)$ is a real-valued function, the subscript t (or x, respectively) denotes the differentiation with respect to the variable t (or x), and $\mathbb{S}$ is the torus of length L. This equation has received increasing interest in this decade. It was first discovered by Fuchssteiner–Fokas [1] with mathematical interest as an example of completely-integrable systems. A decade later, Camassa–Holm [2] (see also [3]) found its physical derivation, and it turned out that the equation models unidirectional propagation of shallow water waves with u representing the fluid velocity in the x direction (or equivalently the height of the fluid's free surface). Slightly after the discovery, in a study of finite-length and small-amplitude waves in cylindrical compressible hyperelastic rods, Dai [4] derived a new nonlinear wave equation similar to the CH. Interestingly, although the physical background is totally different, the Dai equation coincides with the CH with a special choice of parameters. The CH has further interesting features; first, it admits solitary waves that can be peaked (called "peakons"). This is in sharp contrast to other completely-integrable nonlinear wave equations, such as the Korteweg–de Vries equation, where solitary waves are generally smooth. Peakons describe in physical context "wave-breaking" [5] (for shallow water waves), or "rod-breaking" (for rod waves). Second, the equation has a bi-Hamiltonian structure [2]; in other words, the equation can be expressed in two different variational forms as follows. As stated earlier, the CH is completely-integrable, and thus has infinitely many conservation laws. The first three are:

$$G_1(u) = u, \qquad \frac{\mathrm{d}}{\mathrm{d}t}\int_0^L G_1(u)\mathrm{d}x = 0, \tag{2}$$

☆ This work is supported by the 21st Century COE Program on Information Science and Technology Strategic Core, and by the Grant-in-Aid for Encouragement of Young Scientists (B) of the Japan Society for the Promotion of Science.

E-mail address: matsuo@mist.i.u-tokyo.ac.jp.

0377-0427/$ – see front matter © 2009 Elsevier B.V. All rights reserved.
doi:10.1016/j.cam.2009.09.020

$$G_2(u, u_x) = \frac{u^2 + {u_x}^2}{2}, \qquad \frac{\mathrm{d}}{\mathrm{d}t}\int_0^L G_2(u, u_x)\mathrm{d}x = 0, \tag{3}$$

$$G_3(u, u_x) = \frac{u^3 + u{u_x}^2}{2}, \qquad \frac{\mathrm{d}}{\mathrm{d}t}\int_0^L G_3(u, u_x)\mathrm{d}x = 0. \tag{4}$$

Then the CH can be expressed in variational forms with G_2 and G_3 as:

$$\left(1 - \frac{\partial^2}{\partial x^2}\right) u_t = -\frac{\partial}{\partial x}\left(\frac{\delta G_3}{\delta u}\right), \tag{5}$$

and with a new variable $m = (1 - \partial^2/\partial x^2)u$ as

$$m_t = -\left(\frac{\partial}{\partial x}m + m\frac{\partial}{\partial x}\right)\left(\frac{\delta G_2}{\delta m}\right). \tag{6}$$

The symbols $\delta G_3/\delta u$ and $\delta G_2/\delta m$ are variational derivatives, which will be described in the subsequent section. Note that the conservation law (4) (or (3), respectively) is closely related to the variational form (5) (or (6)).

Due to such physical and mathematical relevance, quite much effort have been already devoted to the numerical integration of the CH; for example, several standard pseudospectral schemes [2,3,6], and a finite-difference scheme [7], among many others. Then quite recently the possibility of specialized schemes which fully utilize the geometric structure of the CH has been exploited by several authors; Holden–Raynaud [8] developed a scheme based on the multi-peakon structure of the equation, Cohen–Owren–Raynaud [9] investigated a scheme that preserves the multi-symplecticity of the equation, and Matsuo–Yamaguchi [10] proposed a scheme that strictly conserves the Hamiltonian G_3 by utilizing the variational structure (5). Such structure-preserving schemes are in general expected to be more advantageous (stabler and/or give qualitatively better results) than those based on generic methods, and in fact the expectation is confirmed theoretically and/or numerically in those studies. For more general structure-preserving methods in various contexts, see, for example, a nice review in [11] and references therein (see also [12,13]).

The aim of this paper is to exploit a new possibility of structure-preserving Galerkin scheme for the CH, as somewhat an extension of Matsuo–Yamaguchi [10]. In this work they considered a discrete analogue of the variational form (5), and showed that a scheme based on the discrete variational form successfully preserves Hamiltonian G_3 in some discrete sense. (For related structure-preserving studies on variational PDEs, see [14–16] and references therein.) Then, noticing the bi-Hamiltonian structure, we are naturally guided to a question that how about another Hamiltonian G_2. To express the conclusion first, we can follow the same strategy as in [10] and construct a scheme that strictly preserves G_2. In comparison with the previous study [10], a superiority of the new scheme is that, at least in infinite-precision arithmetic, the scheme is unconditionally stable in the sense that the solution is always bounded.

This paper is organized as follows. In Section 2, the targeted variational structure is briefly reviewed. In Section 3, a G_2-preserving Galerkin scheme is presented following the strategy in [10]. Section 4 is devoted to numerical experiments of the proposed scheme. Finally, in Section 5, some concluding remarks are given.

2. The variational structure and conservation law

In this section the targeted variational structure and its relation to the conservation law is summarized.

Let $L^2(\mathbb{S})$ be the standard L^2 space on $\mathbb{S}$, and $H^j(\mathbb{S})$ be the jth order Sobolev space. Let us also introduce an operator $\mathcal{K} = (1 - \partial^2/\partial x^2)^{-1}$, which is a map $L^2(\mathbb{S}) \to H^2(\mathbb{S})$ [17]. Then, $u = \mathcal{K}m$. Note that, for $f \in H^1(\mathbb{S})$, $(\mathcal{K}f)_x = \mathcal{K}f_x$. With these notations, the Hamiltonian G_2 can be written with m as

$$G_2(\mathcal{K}m, \mathcal{K}m_x) = \frac{(\mathcal{K}m)^2 + (\mathcal{K}m_x)^2}{2}, \tag{7}$$

and its variational derivative with respect to m can be defined. Throughout this section, m is assumed to be sufficiently smooth. By simply differentiating we obtain

$$\begin{aligned}\frac{\mathrm{d}}{\mathrm{d}t}\int_0^L G_2(\mathcal{K}m, \mathcal{K}m_x)\mathrm{d}x &= \int_0^L \left(\frac{\partial G_2}{\partial(\mathcal{K}m)}\cdot\mathcal{K}m_t + \frac{\partial G_2}{\partial(\mathcal{K}m_x)}\cdot\mathcal{K}m_{xt}\right)\mathrm{d}x \\ &= \int_0^L \left(\mathcal{K}\frac{\partial G_2}{\partial(\mathcal{K}m)} - \left(\mathcal{K}\frac{\partial G_2}{\partial(\mathcal{K}m_x)}\right)_x\right) m_t\mathrm{d}x.\end{aligned} \tag{8}$$

Boundary terms are dropped due to the periodicity of m and its derivatives. In light of the equation above, we define the variational derivative by

$$\frac{\delta G_2}{\delta m} :\equiv \mathcal{K}\frac{\partial G_2}{\partial(\mathcal{K}m)} - \left(\mathcal{K}\frac{\partial G_2}{\partial(\mathcal{K}m_x)}\right)_x. \tag{9}$$

It is easy to see that with this particular choice the variational equation (6) coincides with the original equation (1). In fact, since

$$\frac{\partial G_2}{\partial(\mathcal{K}m)} = \mathcal{K}m \quad \text{and} \quad \frac{\partial G_2}{\partial(\mathcal{K}m_x)} = \mathcal{K}m_x, \tag{10}$$

the concrete form of (9) is

$$\frac{\delta G_2}{\delta m} = \mathcal{K}(\mathcal{K}m) - (\mathcal{K}(\mathcal{K}m_x))_x = \mathcal{K}\left(1 - \frac{\partial^2}{\partial x^2}\right)\mathcal{K}m = \mathcal{K}m. \tag{11}$$

Here the trivial identity $(1-\partial^2/\partial x^2)\mathcal{K} = 1$ (the identity map) is used. Substituting this into (6) and using $m = (1-\partial^2/\partial x^2)u$, we obtain (1).

The conservation law (3) directly follows from the skew-symmetry of the operator $\mathcal{J} :\equiv -((\partial/\partial x)m + m(\partial/\partial x))$: for any $f, g \in H^1(\mathbb{S})$,

$$\int_0^L f\mathcal{J}g\,\mathrm{d}x = -\int_0^L (\mathcal{J}f)g\,\mathrm{d}x. \tag{12}$$

This means that the variational PDE (6) is a Hamiltonian PDE, and the corresponding Hamiltonian is conserved. In fact, from (8) we immediately obtain

$$\frac{\mathrm{d}}{\mathrm{d}t}\int_0^L G_2(\mathcal{K}m, \mathcal{K}m_x)\mathrm{d}x = \int_0^L \frac{\delta G_2}{\delta m}m_t\,\mathrm{d}x = \int_0^L \frac{\delta G_2}{\delta m}\cdot\mathcal{J}\frac{\delta G_2}{\delta m}\mathrm{d}x = 0. \tag{13}$$

Observe that the conservation law solely comes from the skew-symmetry of $\mathcal{J}$ and the variational form defined with variational derivative (6), and the concrete form of G_2 is not essential. This enables us to employ the strategy described in the next section.

3. A G_2-conserving Galerkin scheme

In this section we present a G_2-conserving Galerkin scheme. To that end, we commence by defining a new set of weak forms introducing a new intermediate variable p: Find $m(\cdot, t), p \in H^1(\mathbb{S})$ such that for any $v_1, v_2 \in H^1(\mathbb{S})$

$$(m_t, v_1) = (\mathcal{J}p, v_1), \tag{14}$$

$$(p, v_2) = \left(\frac{\partial G_2}{\partial(\mathcal{K}m)}, \mathcal{K}v_2\right) + \left(\frac{\partial G_2}{\partial(\mathcal{K}m_x)}, \mathcal{K}(v_2)_x\right) \tag{15}$$

hold. The brackets $(\cdot,\cdot)$ is the standard inner product in $L^2(\mathbb{S})$. This set of weak forms happily keeps the conservation law as follows.

Theorem 1. *Suppose $m_t(\cdot, t), p \in H^1(\mathbb{S})$. Then the solution m of the weak forms (14), (15) satisfies the conservation law (3).*

Proof. From (8), we see

$$\frac{\mathrm{d}}{\mathrm{d}t}\int_0^L G_2(\mathcal{K}m, \mathcal{K}m_x)\mathrm{d}x = \left(\frac{\partial G_2}{\partial(\mathcal{K}m)}, \mathcal{K}m_t\right) + \left(\frac{\partial G_2}{\partial(\mathcal{K}m_x)}, \mathcal{K}m_{xt}\right) = (p, m_t) = (\mathcal{J}p, p) = 0. \tag{16}$$

The first equality is from (8), the second is from (15) with the assumption $m_t(\cdot, t) \in H^1(\mathbb{S})$, and the third is from (15) with the assumption $p \in H^1(\mathbb{S})$. □

Notice that the variational derivative $\delta G/\delta m$ in the original variational form (6) is now replaced with a set of *partial* derivatives $\partial G/\partial(\mathcal{K}m)$ and $\partial G/\partial(\mathcal{K}m_x)$. Nevertheless, according to the theorem above, the conservation property is kept. Furthermore, the property is again from the skew-symmetry of $\mathcal{J}$ and the (variational) weak forms themselves, and the concrete form of G_2 does not matter. In what follows, we construct a G_2-conserving scheme fully utilizing this point. (For a basic theory on conservative schemes with variational weak forms, see [16]. An extended example for the CH, which deals with a G_3-conserving scheme, is given in [10]).

We denote the approximate solutions by $m^{(n)} \simeq m(\cdot, n\Delta t)$ and $p^{\left(n+\frac{1}{2}\right)} \simeq p(\cdot, \left(n+\frac{1}{2}\right)\Delta t)(n = 0, 1, 2, \ldots)$, where Δt is the time mesh size. To mimic the variational weak forms (14), (15), we first define a discrete version of G_2 by

$$G_{\mathrm{d}}(\mathcal{K}m^{(n)}, \mathcal{K}m_x^{(n)}) :\equiv \frac{(\mathcal{K}m^{(n)})^2 + (\mathcal{K}m_x^{(n)})^2}{2}. \tag{17}$$

Below this will be often abbreviated as ${G_{\mathrm{d}}}^{(n)}$ for saving space. We then define associated discrete partial derivatives by

$$\frac{\partial G_{\mathrm{d}}}{\partial(\mathcal{K}m^{(n+1)}, \mathcal{K}m^{(n)})} :\equiv \mathcal{K}m^{\left(n+\frac{1}{2}\right)}, \qquad \frac{\partial G_{\mathrm{d}}}{\partial(\mathcal{K}m_x^{(n+1)}, \mathcal{K}m_x^{(n)})} :\equiv \mathcal{K}m_x^{\left(n+\frac{1}{2}\right)}, \tag{18}$$

where $m^{\left(n+\frac{1}{2}\right)} :\equiv (m^{(n+1)} + m^{(n)})/2$. They apparently approximate the continuous case (10), and it is easy to check that they satisfy the following discrete chain rule corresponding to (8).

$$\frac{1}{\Delta t}\int_0^L \left(G_{\mathrm{d}}{}^{(n+1)} - G_{\mathrm{d}}{}^{(n)}\right) \mathrm{d}x = \left(\frac{\partial G_{\mathrm{d}}}{\partial(\mathcal{K}m^{(n+1)}, \mathcal{K}m^{(n)})}, \mathcal{K}\left(\frac{m^{(n+1)} - m^{(n)}}{\Delta t}\right)\right) + \left(\frac{\partial G_{\mathrm{d}}}{\partial(\mathcal{K}m_x^{(n+1)}, \mathcal{K}m_x^{(n)})}, \mathcal{K}\left(\frac{m_x^{(n+1)} - m_x^{(n)}}{\Delta t}\right)\right). \tag{19}$$

With the discrete partial derivatives, a scheme is defined as follows. Let S_1, S_2 be some appropriate trial spaces, and W_1, W_2 test spaces. We define an operator

$$\mathcal{J}^{\left(n+\frac{1}{2}\right)} :\equiv -\left(\frac{\partial}{\partial x}m^{\left(n+\frac{1}{2}\right)} + m^{\left(n+\frac{1}{2}\right)}\frac{\partial}{\partial x}\right), \tag{20}$$

which approximates $\mathcal{J}$, and is skew-symmetric.

Scheme 3.1 (G_2-*Conserving Scheme*). *Find* $m^{(n)} \in S_2$ *and* $p^{\left(n+\frac{1}{2}\right)} \in S_1$ $(n = 0, 1, 2, \ldots)$ *such that for any* $v_1 \in W_1$ *and* $v_2 \in W_2$,

$$\left(\frac{m^{(n+1)} - m^{(n)}}{\Delta t}, v_1\right) = \left(\mathcal{J}^{\left(n+\frac{1}{2}\right)}p^{\left(n+\frac{1}{2}\right)}, v_1\right), \tag{21}$$

$$\left(p^{\left(n+\frac{1}{2}\right)}, v_2\right) = \left(\frac{\partial G_{\mathrm{d}}}{\partial(\mathcal{K}m^{(n+1)}, \mathcal{K}m^{(n)})}, \mathcal{K}v_2\right) + \left(\frac{\partial G_{\mathrm{d}}}{\partial(\mathcal{K}m_x^{(n+1)}, \mathcal{K}m_x^{(n)})}, \mathcal{K}(v_2)_x\right). \tag{22}$$

hold. □

Then the scheme enjoys the following conservation property. Observe that the proof goes exactly the same way as in the continuous case.

Theorem 2 (*Discrete* G_2-*Conservation Law*). *Suppose* $(m^{(n+1)} - m^{(n)})/\Delta t \in W_2$ $(n = 0, 1, 2, \ldots)$ *and* $S_1 \subseteq W_1$. *Then Scheme* 3.1 *is conservative in the sense that*

$$\frac{1}{\Delta t}\int_0^L \left(G_{\mathrm{d}}{}^{(n+1)} - G_{\mathrm{d}}{}^{(n)}\right) \mathrm{d}x = 0 \quad (n = 0, 1, 2, \ldots) \tag{23}$$

holds. □

Proof. From the discrete chain rule (19),

$$\begin{aligned}\frac{1}{\Delta t}\int_0^L \left(G_{\mathrm{d}}{}^{(n+1)} - G_{\mathrm{d}}{}^{(n)}\right) \mathrm{d}x &= \left(\frac{\partial G_{\mathrm{d}}}{\partial(\mathcal{K}m^{(n+1)}, \mathcal{K}m^{(n)})}, \mathcal{K}\left(\frac{m^{(n+1)} - m^{(n)}}{\Delta t}\right)\right) \\ &\quad + \left(\frac{\partial G_{\mathrm{d}}}{\partial(\mathcal{K}m_x^{(n+1)}, \mathcal{K}m_x^{(n)})}, \mathcal{K}\left(\frac{m_x^{(n+1)} - m_x^{(n)}}{\Delta t}\right)\right) \\ &= \left(p^{\left(n+\frac{1}{2}\right)}, \frac{m_x^{(n+1)} - m_x^{(n)}}{\Delta t}\right) \\ &= \left(\mathcal{J}^{\left(n+\frac{1}{2}\right)}p^{\left(n+\frac{1}{2}\right)}, p^{\left(n+\frac{1}{2}\right)}\right) \\ &= 0.\end{aligned} \tag{24}$$

In the second and third equality, the assumptions are used. The last equality follows from the skew-symmetry of $\mathcal{J}^{\left(n+\frac{1}{2}\right)}$. □

The trial and test function spaces can be set to various standard ones such as the standard finite-dimensional Fourier space or the finite-element spaces, depending on the users' preferences. Theorem 2 clarifies the conditions for the scheme to be successfully conservative. The simplest and most useful choice would be the use of the standard periodic piecewise-linear function space on some fixed grid for all of S_1, S_2, W_1 and W_2; in that case, the assumptions in the theorem are trivially satisfied.

An important outcome of preserving the G_2-conservation law is that Scheme 3.1 gains the following stability property. Let us denote the approximate solution of u by $u^{(n)} :\equiv \mathcal{K}m^{(n)}$.

Theorem 3 (*Stability of* Scheme 3.1). *Scheme* 3.1 *is stable in the sense that (in exact arithmetic)* $\|u^{(n)}\|_\infty < \infty$ $(n = 0, 1, 2, \ldots)$.

Proof. From the G_2-conservation, we readily see that there exists a constant c such that

$$\|u^{(n)}\|_\infty \le c\|u^{(n)}\|_{H^1(\mathbb{S})} = \text{const.}, \tag{25}$$

by the Sobolev lemma. □

4. Implementation issues and numerical experiments

After briefly mentioning on the implementation issues, some numerical experiments are given in order to confirm the theory and effectiveness of the proposed scheme. Throughout this section, the equispaced spatial mesh of N grid points $(x_0 = 0, x_N = L)$ is assumed, and the standard periodic piecewise-linear function space on the mesh, denoted as S_p, is used as the trial and test spaces. The basis functions are denoted by $\phi_k(x)$ $(k = 0, \ldots, N-1)$.

4.1. Implementation issues

In actual computation, the inverse operator $\mathcal{K} = (1 - \partial^2/\partial x^2)^{-1}$ is realized as the convolution

$$(\mathcal{K}f)(x) = (k * f)(x) = \int_0^L k(x-\xi)f(\xi)\mathrm{d}\xi, \tag{26}$$

with the Green function:

$$k(x) = \frac{\cosh(x - L[x/L] + L/2)}{2\sinh(L/2)}. \tag{27}$$

The operator appears in the second equation of Scheme 3.1, which reads

$$\left(p^{\left(n+\frac{1}{2}\right)}, v_2\right) = \left(\mathcal{K}m^{\left(n+\frac{1}{2}\right)}, \mathcal{K}v_2\right) + \left(\mathcal{K}m_x^{\left(n+\frac{1}{2}\right)}, \mathcal{K}(v_2)_x\right). \tag{28}$$

If we introduce the matrices

$$A_{ij} :\equiv (\phi_i, \phi_j), \qquad (K_1)_{ij} :\equiv \left(\mathcal{K}\phi_i, \mathcal{K}\phi_j\right), \quad \text{and} \quad (K_2)_{ij} :\equiv \left(\mathcal{K}(\phi_i)_x, \mathcal{K}(\phi_j)_x\right), \tag{29}$$

then the concrete form of Scheme 3.1 becomes

$$A\left(\frac{\boldsymbol{m}^{(n+1)} - \boldsymbol{m}^{(n)}}{\Delta t}\right) = \boldsymbol{g}\left(\boldsymbol{m}^{\left(n+\frac{1}{2}\right)}, \boldsymbol{p}^{\left(n+\frac{1}{2}\right)}\right), \tag{30}$$

$$A\boldsymbol{p}^{\left(n+\frac{1}{2}\right)} = K_1\boldsymbol{m}^{\left(n+\frac{1}{2}\right)} + K_2\boldsymbol{m}^{\left(n+\frac{1}{2}\right)}, \tag{31}$$

where $\boldsymbol{m}^{(n)} :\equiv (m_0^{(n)}, \ldots, m_{N-1}^{(n)})^\mathrm{T}$, $\boldsymbol{m}^{\left(n+\frac{1}{2}\right)} :\equiv (\boldsymbol{m}^{(n+1)} + \boldsymbol{m}^{(n)})/2$, $\boldsymbol{p}^{\left(n+\frac{1}{2}\right)} :\equiv (p_0^{(n)}, \ldots, p_{N-1}^{(n)})^\mathrm{T}$, and $\boldsymbol{g}$ is the vector function that represents the nonlinear part in the first equation (we omit the concrete form of $\boldsymbol{g}$ here, since it is straightforward and not important for the discussion here). The equations above is a system of nonlinear and linear equations of dimension $2N$, but can be readily reduced to

$$A\left(\frac{\boldsymbol{m}^{(n+1)} - \boldsymbol{m}^{(n)}}{\Delta t}\right) = \boldsymbol{g}\left(\boldsymbol{m}^{\left(n+\frac{1}{2}\right)}, A^{-1}(K_1 + K_2)\boldsymbol{m}^{\left(n+\frac{1}{2}\right)}\right), \tag{32}$$

which is of dimension N; that is, the intermediate variable $\boldsymbol{p}^{\left(n+\frac{1}{2}\right)}$ can be erased in actual computation. Note that the matrices A, K_1 and K_2 depend only on the grid and basis functions, and can be computed *in prior to* time evolution process; heavy convolutions are not required during the main computation. In the numerical experiment below, at each time step the Eq. (32) is solved by the hybrid Newton algorithm `imsl_d_zeros_sys_eqn` in the IMSL library.

Since the time integration is solely carried out in m space, we have to switch from/to the original variable u as pre- and post-processes. Let N_t be the number of temporal time steps. Then the overall integration procedure is as follows.

(i) For a given initial data $u(x, 0)$, compute $m(x, 0) = (1 - \partial^2/\partial x^2)u(x, 0)$;
(ii) Time integration: repeat $m^{(n+1)} \leftarrow m^{(n)}$ $(n = 0, 1, 2, \ldots)$ by (32);
(iii) For the obtained final data $m^{(N_t)}(x)$, compute $u^{(N_t)} = \mathcal{K}m^{(N_t)}$ as the solution.

Note that when we need the approximate solution in the form of u, we have to compute the convolution $\mathcal{K}m^{(n)}$, which is relatively time-consuming. Usually, however, we need u itself at relatively few time steps compared to the whole number of computation steps, and the additional cost is considered to be acceptable in practical situations.

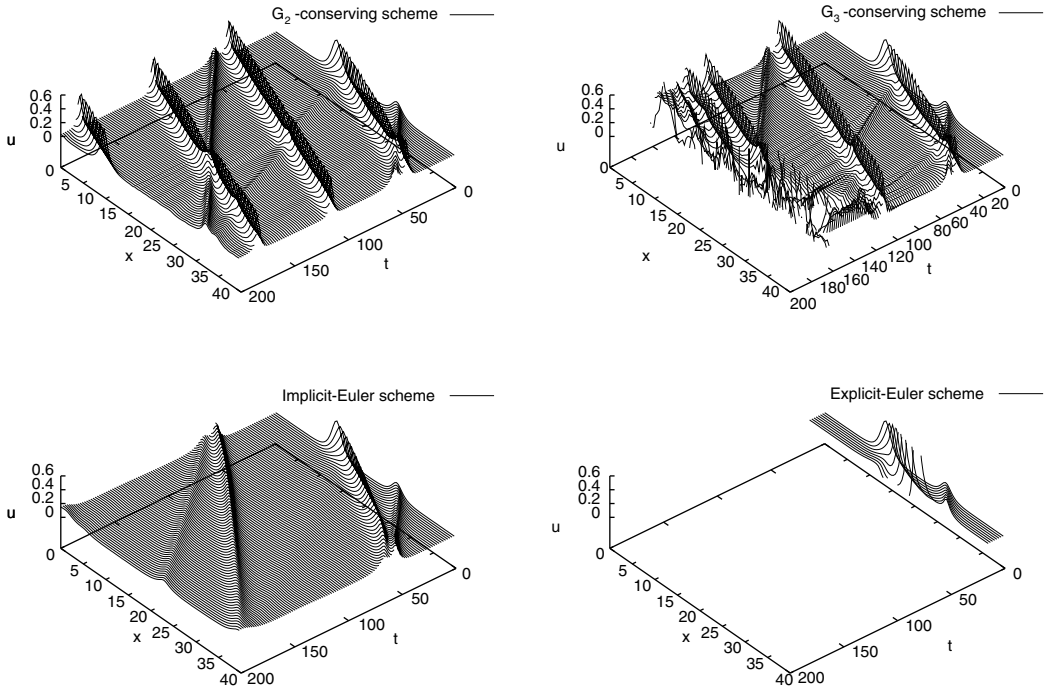

Fig. 1. Evolution of the numerical solutions: (top-left) the proposed G_2-conserving scheme, (top-right) the G_3-conserving scheme, (bottom-left) the implicit-Euler scheme, (bottom-right) the explicit-Euler scheme.

4.2. Numerical experiments

We consider the collision of two soliton-like solutions as an illustrative example. We set $L = 40$, which is divided into $N = 100$ grids. The initial data is set to $u(x, 0) = 0.2\,\mathrm{sech}(x - 403/15) + 0.5\,\mathrm{sech}(x - 203/15)$. Then the problem is integrated in the time interval $[0, 200]$, with the time mesh size $\Delta t = 0.1$ (i.e. the number of temporal grids $N_t = 2000$). In addition to the proposed Scheme 3.1, we also tested for comparison an implicit-Euler scheme:

$$\left(\frac{m^{(n+1)} - m^{(n)}}{\Delta t}, v_1\right) = \left(-\left(\frac{\partial}{\partial x} m^{(n+1)} + m^{(n+1)} \frac{\partial}{\partial x}\right) p^{\left(n+\frac{1}{2}\right)}, v_1\right), \quad \forall v_1 \in S_{\mathrm{p}} \tag{33}$$

$$\left(p^{\left(n+\frac{1}{2}\right)}, v_2\right) = \left(\mathcal{K} m^{(n+1)}, \mathcal{K} v_2\right) + \left(\mathcal{K} m_x^{(n+1)}, \mathcal{K}(v_2)_x\right), \quad \forall v_2 \in S_{\mathrm{p}}, \tag{34}$$

an explicit-Euler scheme:

$$\left(\frac{m^{(n+1)} - m^{(n)}}{\Delta t}, v_1\right) = \left(-\left(\frac{\partial}{\partial x} m^{(n)} + m^{(n)} \frac{\partial}{\partial x}\right) p^{\left(n+\frac{1}{2}\right)}, v_1\right), \quad \forall v_1 \in S_{\mathrm{p}} \tag{35}$$

$$\left(p^{\left(n+\frac{1}{2}\right)}, v_2\right) = \left(\mathcal{K} m^{(n)}, \mathcal{K} v_2\right) + \left(\mathcal{K} m_x^{(n)}, \mathcal{K}(v_2)_x\right), \quad \forall v_2 \in S_{\mathrm{p}} \tag{36}$$

and the G_3-conserving scheme proposed in [10]. Note that the implicit-Euler and explicit-Euler schemes above are also based on the conservative weak forms (14), (15), but all $m^{\left(n+\frac{1}{2}\right)}$'s in Scheme 3.1 are replaced with $m^{(n+1)}$ or $m^{(n)}$, and thus the conservation law is lost in those cases. Note also that the computational complexity of the implicit-Euler scheme is almost the same as that of Scheme 3.1.

Fig. 1 shows the evolution of the approximate solutions. In the result by the proposed scheme (top-left figure), the collisions of the two soliton-like solutions are rightly captured; the larger (thus faster) soliton-like solution overtakes the smaller (slower) one as expected. The computation proceeded quite stably. The implicit-Euler scheme (bottom-left) is favorably stable as well, but the stability rather comes from the strong dissipation property that is often observed in general implicit-Euler schemes; in fact, the solution rapidly gets flattened. As a consequence, the soliton-like solutions get slower (recall that the speed of a soliton-like solution depends on its size), and the larger solution goes round the interval only once, instead of three times originally expected. Thus the implicit-Euler scheme should be rejected, when the qualitative behavior of the problem is of our interest. The explicit-Euler scheme (bottom-right) is quite unstable as expected, and the solution blows up soon after the start of computation. This scheme does not deserve further consideration. On the result

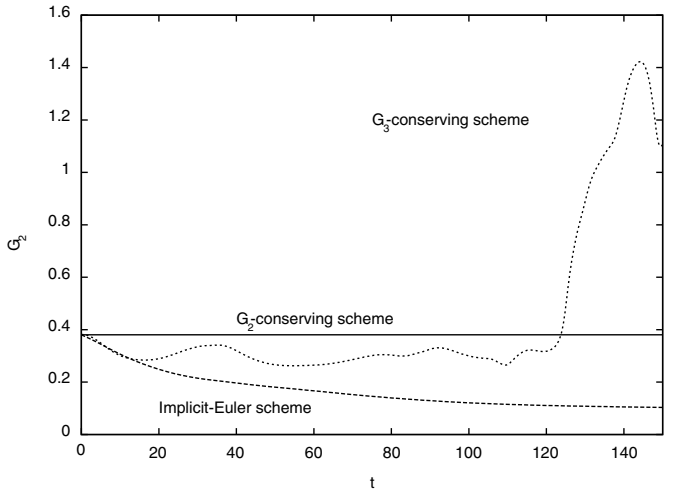

Fig. 2. Evolution of G_2.

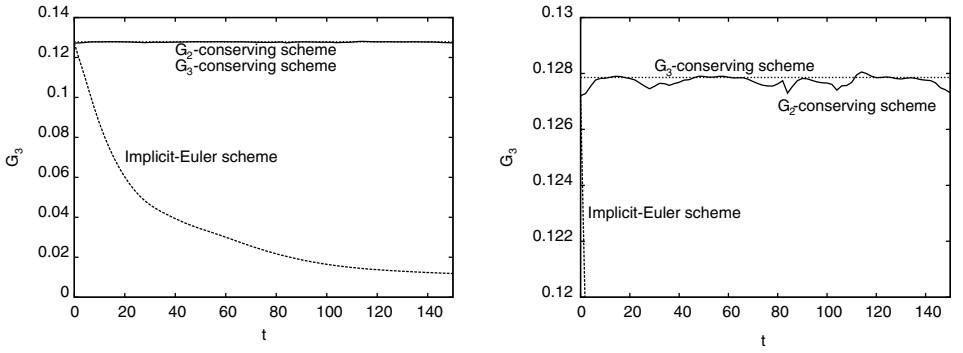

Fig. 3. Evolution of G_3: (left) overall profile (right) details.

by the G_3-conserving scheme (top-right), some careful discussion is required. In the early phase of computation (more precisely speaking, at least until around $t = 100$), it happily captures the collision process and the qualitative behavior agrees with that of G_2-conserving scheme. After that, however, the solution shows instability. The difference between the G_2- and G_3-conserving schemes in terms of stability should be attributed to the additional stability property of the G_2-conserving scheme stated in Theorem 3. In this sense, we can say that the property is of practical importance. (Note that the result here does not immediately imply that the G_3-conserving scheme is unstable; it has been confirmed in [10] that the G_3-conserving scheme is actually stabler than several generic schemes. The result just claims the G_2-conserving one is further better).

The evolutions of the invariants G_2 and G_3 in each scheme (except the explicit-Euler scheme) are shown in Figs. 2 and 3. In Fig. 2, we can see that the G_2-conserving scheme rightly conserves G_2, while the other two schemes fail. In the implicit-Euler scheme, G_2 is steadily dissipated. In the G_3-conserving scheme, G_2 stays around the exact value in the early phase of evolution, but finally it nearly blows up; this corresponds to the instability observed in Fig. 1. The graphs in Fig. 3 show the evolution of G_3; the left figure shows the overall profile, and the right shows its detail around the true G_3 value, which is to clarify the difference between the G_2- and G_3-conserving schemes. According to the graphs, in the implicit-Euler scheme G_3 is again soon dissipated. The G_3-conserving scheme strictly conserves the invariant as the theory suggests, while the G_2-conserving scheme *nearly* conserves it.

Finally, the G_2-conserving scheme is checked on coarser meshes $N = 20$ (i.e. $\Delta x = 2$) and $N = 40$ ($\Delta x = 1$), in order to check if the scheme is stable with respect to the spatial discretization. The time mesh size is kept the same ($\Delta t = 0.1$). Fig. 4 shows the results, which suggest that the scheme is stable even with very coarse mesh.

5. Concluding remarks

In this paper a new G_2-conserving Galerkin scheme has been presented for the Camassa–Holm (CH) equation. To the best of the author's knowledge, this is the first G_2-conserving Galerkin scheme so far. The scheme has been confirmed with

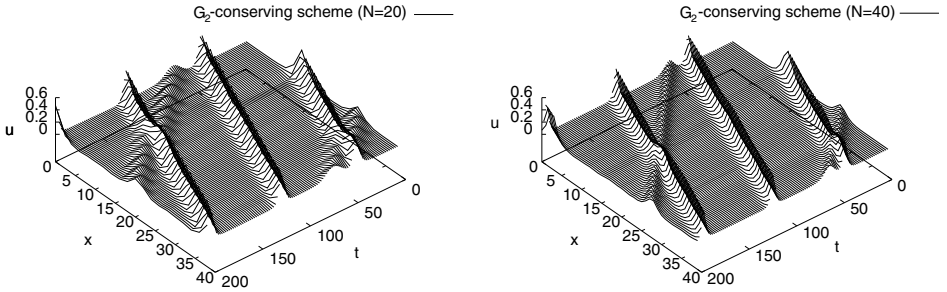

Fig. 4. Evolution of the numerical solutions on coarser meshes with the G_2-conserving scheme: (left) $N = 20$ (right) $N = 40$.

a simple numerical experiment. It should be also noted that in the proposed scheme adaptive time-stepping technique can be incorporated (note that Theorem 2 involves only the time steps n and $(n+1)$, and Δt can be changed at every time steps).

We would like to add some discussion on the comparison of the two conservative schemes; the G_2- and G_3-conserving schemes. The theories and numerical experiments show that these schemes strictly preserve the aimed invariants, and at the same time, fail to keep the other ones. Then arise natural questions—which one is better? And is it impossible to preserve *both* of them? The authors feel they are questions common to many conservative problems with multiple invariants; for example, the Korteweg–de Vries equation has infinitely many invariants, and many conservative schemes, each of which preserves a specific invariant, have been proposed. As far as the author know, however, no clear answer has been given to the above questions. Turning back to the CH, we can only say that from functional analytic view, the invariant G_2 yields the stability in $\|\cdot\|_\infty$, at least in exact arithmetic, and thus gives us a strong reason to choose it. In fact in the present paper it is numerically confirmed that the G_2-conserving scheme is stabler than the other schemes. The scheme has, however, a potential drawback compared to the G_3-conserving scheme that since it is formulated in the variable $m = (1 - \partial^2/\partial x^2)u$, it can capture only H^3 (when $m \in H^1$) or smoother solutions in terms of the original variable u; this is not a good news when peakons are the main target of the calculation. This problem does not occur in the G_3-conserving scheme, which is formulated in u and allows its H^1 approximations. Thus a natural conclusion would be that the G_2-conserving scheme is preferable when smooth solutions are the main target, since its allows stable computation with larger time steps. Otherwise, the G_3-conserving scheme with more moderate time stepping would be a better choice.

We would like to conclude this paper by listing up possible future works. First, more rigorous mathematical argument on the above issue is hoped. Second, the conservative Galerkin schemes should be compared with other structure-preserving schemes for the equation; for example, the multi-symplectic scheme proposed in [9]. We should also note that for quadratic invariants, there is a generic method in the literature for constructing conservative finite-difference schemes; an appropriate spatial discretization which results in a Hamiltonian system of ODEs (see, for example, McLachlan–Robidoux [18]), followed by several Runge–Kutta methods such as the Gauss–Legendre RK methods [13], would automatically conserve the targeted quadratic invariant. It seems even possible to utilize nonuniform spatial grids in the finite-difference context [19]. Comparisons among these structure-preserving schemes must be carefully done in view of efficiency and qualitative behavior of solutions.

Acknowledgements

The author would like to thank the anonymous reviewers for valuable comments. Part of this work is supported by a Grant-in-Aid of the Ministry of Education, Culture, Sports, Science and Technology of Japan, and by the Global Center of Excellence "The research and training center for new development in mathematics".

References

[1] B. Fuchssteiner, A.S. Fokas, Symplectic structures, their Bäcklund transformations and hereditary symmetries, Physica D 4 (1981) 47–66.
[2] R. Camassa, D.D. Holm, An integrable shallow water equation with peaked solitons, Phys. Rev. Lett. 71 (1993) 1661–1664.
[3] R. Camassa, D.D. Holm, J.M. Hyman, A new integrable shallow water equation, Adv. Appl. Mech. 31 (1994) 1–33.
[4] H.H. Dai, Model equations for nonlinear disperwive waves in a compressible Mooney–Rivlin Rod, Acta Mech. 127 (1998).
[5] G.B. Whitham, Linear and Nonlinear Waves, John Wiley & Sons, New York, 1974.
[6] H. Kalische, J. Lenells, Numerical study of traveling-wave solutions for the Camassa–Holm equation, Chaos Solitons Fractals 25 (2005) 287–298.
[7] H. Holden, X. Raynaud, A convergent numerical scheme for the Camassa–Holm equation based on multipeakons, Discrete Contin. Dyn. Syst. 14 (2006) 505–523.
[8] H. Holden, X. Raynaud, Convergence of a finite difference scheme for the Camassa–Holm equation, SIAM J. Numer. Anal. 44 (2006) 1655–1680.
[9] D. Cohen, B. Owren, X. Raynaud, Multi-symplecetic integration of the Camassa–Holm equation, J. Comput. Phys. 227 (2008) 5492–5512.
[10] T. Matsuo, H. Yamaguchi, An energy-conserving Galerkin scheme for a class of nonlinear dispersive equations, J. Comput. Phys. 228 (2009) 4346–4358.
[11] C.J. Budd, M.D. Piggott, Geometric Integration and its Applications, in: Handbook of Numerical Analysis, vol. XI, North-Holland, Amsterdam, 2003, pp. 35–139.
[12] B. Leimkuhler, S. Reich, Simulating Hamiltonian Dynamics, Cambridge University Press, Cambridge, 2004.
[13] E. Hairer, C. Lubich, G. Wanner, Geometric Numerical Integration: Structure-Preserving Algorithms for Ordinary Differential Equations, 2nd ed., Springer-Verlag, Berin, 2006.

[14] D. Furihata, Finite difference schemes for $\frac{\partial u}{\partial t} = (\frac{\partial}{\partial x})^{\alpha} \frac{\delta G}{\delta y}$ that inherit energy conservation or dissipation property, J. Comput. Phys. 156 (1999) 181–205.
[15] T. Matsuo, D. Furihata, Dissipative or conservative finite difference schemes for complex-valued nonlinear partial differential equations, J. Comput. Phys. 171 (2001) 425–447.
[16] T. Matsuo, Dissipative/conservative Galerkin method using discrete partial derivatives for nonlinear evolution equations, J. Comput. Appl. Math. 218 (2008) 506–521.
[17] H. Brezis, Analyse Fonctionnelle, Masson, Paris, 1983.
[18] R.I. McLachlan, N. Robidoux, Antisymmetry, pseudospectral methods, and conservative PDEs, in: International Conference on Differential Equations, Vol. 1, 2, World Sci. Publ., River Edge, NJ, 2000, pp. 994–999. (Berlin, 1999).
[19] R.I. McLachlan, Spatial discretization of partial differential equations with integrals, IMA J. Numer. Anal. 23 (2003) 645–664.